Structural Engineering and Mechanics, *Vol. 73, No. 4 (2020) 381-395*
DOI: https://doi.org/10.12989/sem.2020.73.4.381

Analysis of behavior of bare and in-filled RC frames subjected to quasi static loading

Balvir Sandhu[1a], Shruti Sharma[*1] and Naveen Kwatra[1b]

Department of Civil Engineering, Thapar University, Patiala, Punjab, India-147004

(Received November 12, 2018, Revised July 18, 2019, Accepted August 27, 2019)

Abstract. Study on the inelastic response of bare and masonry infilled Reinforced Concrete (RC) frames repaired using Carbon Fibre Reinforced Polymers (CFRP) and Glass Fiber Reinforced Polymers (GFRP) subjected to quasi- static loading is presented in the work. The hysteresis behaviour, stiffness retention, energy dissipation and damage index are the parameters employed to analyze the efficacy of FRP strengthening of bare and brick in-filled RC frames. It is observed that there is a significant improvement in load carrying capacity of brick infilled frame over bare RC frame. Also FRP strengthened brick infilled frame performs much better than FRP repaired bare frame under quasi static loading. Repair and retrofitting of brick infilled RC frame shows an improved load carrying and damage tolerance capacity than control frame.

Keywords: retrofitting; RC frame; brick infill; damage index; GFRP; CFRP; FRF

1. Introduction

While modeling a Reinforced Concrete (RC) framed structure, usually a bare frame is modeled and the infill walls present in the frame are ignored (Nav *et al.* 2016, Yang *et al.* 2017, Singh *et al.* 2017). Most of the research has concentrated on the seismic behaviour of FRP retrofitting of masonry wall assemblages and very few of them focused on the retrofitting of infilled RC frames (Massumi and Mohamaddi 2016). Practically, the infill walls provide higher stiffness and strength for the frames. But their effect on the structure performance is ignored due to lack of adequate information about the behaviour of frame with infill walls. Masonry infills are frequently used in RC frames in form of interior partition wall and exterior walls as a large proportion of total mass of the frame. Masonry infill walls in frame structures have been long known to affect the strength and stiffness of the infilled frame structures. The masonry infill material is anisotropic material having wide range of deformation strength and energy dissipation properties. They can be thought as the weak links in the RC structure and so are liable to failure especially due to lateral displacement during a strong ground motion which can cause severe damage to the infilled frame. It can be attributed to the poor shear and tensile strength leading to the brittleness of the brick infill. In seismic zones, ignoring the frame–wall interaction is not always on the safe side, because under lateral loads, the infill walls show increased stiffness. This increased stiffness can further results in change in the seismic demand due to the significant reduction in the natural period of the composite structural system. The composite action of the frame–wall system changes the magnitude and the distribution of straining actions in the frame members, i.e., critical sections in the infilled frame differ from those in the bare frame, which may lead to un-conservative or poorly detailed designs.

If the structure has been damaged either due to poor or faulty design or earthquake resistant deficiencies, it is required to repair or retrofit the structure. Generally retrofitting of these types of buildings include addition of new members such as shear wall and bracing and/or strengthening existing members by FRP like GFRP and CFRP, Steel or RC jacketing. Chang *et al.* (2004) found that the strength and ductility of the CFRP repaired bridge column may be largely restored after the CFRP composite sheets are engaged and external confinement is developed at larger lateral displacements. Memon and Sheikh (2005) concluded that the overall ductile performance depends on the extent of damage sustained by the specimens prior to being wrapped with GFRP. Yuksel *et al.* (2010) conducted an experimental and results showed a significant increase in the yield and ultimate strength capacities of the frames with a decrease in relative story drifts, especially in the cross-braced and the cross diamond-braced of retrofitting schemes. Lakshmikandhan *et al.* (2012) presented the behaviour of Retrofitted beam from the experimental and analytical studies. The result is shown that the width and stiffness of CFRP affected the failure modes of retrofitted beams. The increase of CFRP stiffness has increased the maximum load to a certain value, thereafter the stiffness increase resulted in decreases of load capacity.

Cho *et al.* (2008) presented a non-linear model of reinforced concrete frames retrofitted by in-filled HPFRCC walls. Lakshmikandhan *et al.* (2013) revealed that the

∗Corresponding author, Professor
E-mail: shruti.sharma@thapar.edu
[a] Ph.D. Student
E-mail: sandhu_balvir@yahoo.co.in
[b] Professor
E-mail: nkwatra@thapar.edu

ISSN: 1225-4568 (Print), 1598-6217 (Online)

repaired damaged beams outperformed than the undamaged control beam strengthened with CFRP. Ozkaynak *et al.* (2014) investigated the equivalent damping ratio of carbon fiber reinforced polymer retrofitted in filled RC systems through a series of 1/3-scaled, one-bay, one-story frames. The equivalent damping for bare frame varied between 8-11% and for infilled frame it was 13 % depending on the damage level. Sathiaseelan and Arulselvan (2015) concluded that the frames damaged due to earthquake can be retrofitted effectively by the application of Ferro cement with cement mortar grouting. The application of Ferro cement technique is a cost effective one and can be executed with less skilled labour. Beydokhty and Shariatmadar (2016) conducted some tests on FRP strengthening technique of damaged beam-column joints. The performance level of damaged joints under cyclic tests was also improved. The repair ability level of damage was also evaluated up to 1.5% drift ratio for tested Beam-Column joints. Tunaboyu and Avsar (2017) carried out the seismic repair of captive-column damage with CFRPs in sub-standard RC frames.

Structural health monitoring (SHM) using various existing techniques provides a means to assess the structural integrity and properties of existing structures in all aspect. Damage detection using vibration measurement of dynamic properties such as natural frequency, mode shape and frequency response function is non-destructive technique and it is widely used to monitor the damage of structure. Several researchers have relied on the use of vibration measurement for system identification and damage detection. Vibration responses of structures are related to structural weaknesses associated with resonance behavior, e.g., natural frequencies are being excited by operational forces. The complete dynamic behavior of a structure in a given frequency range can be viewed as a set of individual modes of vibration. Each result has a characteristic natural frequency, damping, and mode shape. By using these so-called modal parameters to model the structure, problems such as specific resonances can be examined and subsequently solved.

To know the extent of damage in a structure, damage assessment is necessary which is done by calculating the damage index. This index depends upon the specific damage parameters such as structural stiffness, strength degradation, stiffness degradation, deformation, energy dissipation and dynamic properties of structure. Different scientists developed different damage indexes depending upon the specific damage parameters. The well known combined damage index method was proposed by Park and Ang (1985). This index is calculated as a linear combination of maximum displacement response and total hysteretic energy dissipation under cyclic load. However, this damage index is not able to monitor the damage of retrofitted structure in proper way because cracks are covered by strengthening material layers.

Damage detection using vibration measurement of dynamic properties, such as natural frequency, mode shape and frequency response function (FRF), is nondestructive technique and it has widely used to monitor the damage of structure. Several researchers have relied on the use of vibration measurement for system identification and damage detection. Dipasquale and Cakmak (1990) presented a damage index based on the change of frequency ratios. This method considers fundamental structural frequencies before and after damage. It was observed that new vibration signature obtained during a routine operation deviates from that of the baseline value, the building should be checked for possible local defects (Yao *et al.* 1992). These dynamic characteristics can be measured directly by vibrating a structure using digital signal processing equipment and Fast Fourier Transform (FFT) routines (Rao 2000). Damage detection by calculating the change in modal parameters, such as natural frequency, mode shape, and frequency response function (FRF), are also non-destructive techniques that are widely used. Ko *et al.* (2002) developed the Modal Flexibility Damage Index. This index compares flexibility matrices from two sets of mode shapes. Maia *et al.* (2003) presented an FRF-based mode shape method that uses FRF data taken directly from structures without any intermediate steps. Typical vibration identification assumes that the dynamic property of a structure is a sensitive indicator of its physical integrity. When any of the properties like mass, stiffness, or damping of the structure changes due to a structural defect, the vibration response of the structure will also change (Kanwar *et al.* 2006, Goyal 2007, Vimuttasoongviriya *et al.* 2009). Kanwar *et al*. (2016) concluded that the magnitude of FRF decreases with the increase in the level of damage in the RC building model. There is large reduction (more than 50%) in FRF magnitude at state of first visible crack. The magnitude of FRF varies with the level of damage in the storey. The FRF magnitude in the severely damaged storey has been observed to be the minimum.

In this study a bare and a masonry infilled RC frame were subjected to cyclic loading to failure and difference in their structural behavior was reported. Further bare and brick infilled RC frames were repaired using FRP and the effect of FRP strengthening on two frames was studied. This research work mainly focuses on the comparison of behavior of control RC frame, FRP repaired bare RC frame and FRP repaired masonry infilled RC frame subjected to cyclic loading. Various parameters such as load carrying capacity, stiffness retention, energy dissipation and dynamic properties have been considered to evaluate the vis-a-vis performance of different frames. Dynamic properties were used to define the damage tolerance capacity.

2. Experimental details

2.1 Bare and masonry in-filled RC frame

For studying inelastic behavior of seismically damaged bare RC frame and masonry infilled RC frame repaired with FRP, a three storied scaled down (scale factor = 1/3) frames was constructed with concrete using design mix proportions of 1 :1.4: 2.8 (cement: sand: aggregates) and Fe500 steel. The average compressive strength of the concrete used 22.46 MPa after 28 days of curing (Table 1). The cross section of the columns was 100mm square reinforced with 4 # 8 mm Ø bars and with a floor-to-floor height of 950 mm. All beams were rectangular with a cross section size of 100 mm × 150 mm reinforced with 2#10 mm Ø bars @ top and

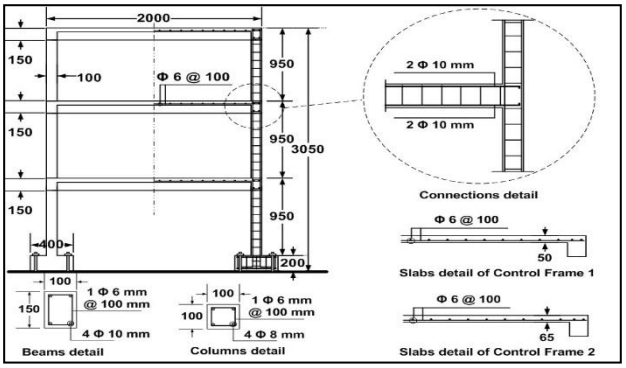

Fig. 1 Reinforcement details of RC frame

Fig. 2 Actual RC Bare Frame used in the study

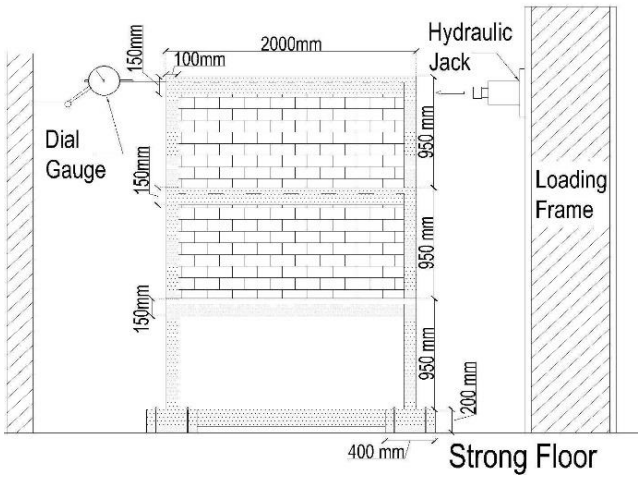

Fig. 3 RC masonry infilled frame test

bottom. All columns and beams were provided with 6 mm diameter stirrups at 100 mm center to center spacing (Fig.1). Each column was cast integrally with stub foundation, which was in turn bolted firmly with the strong floor and connected with plinth beam of size 150mm × 100mm in bare frame (Fig. 2). In masonry infilled frame, first storey was designed as soft storey simulating a multistoried building with parking space and second and third storey were constructed with masonry infills (Fig. 3). 1:4 cement mortar was used in brick masonry. Top floor

Table 1 Properties of Materials used

Compressive strength of Concrete		
Structural elements	Compressive Strength (MPa)	Standard Deviation
First storey	24.20	1.48
Second storey	20.84	1.89
Third storey	23.01	1.87
Average	22.46	1.74
Tensile Strength of Steel used		
Steel size	Yield strength (MPa)	Tensile strength (MPa)
10 mm-diameter	490.18	586.60
8 mm-diameter	523.43	628.91
6 mm-diameter	517.87	636.36
Properties of GFRP and CFRP		
Property	GFRP	CFRP
Tensile strength (GPa)	3.4	4.137
Elastic modulus (GPa)	63	242
Density (g/cm^3)	2.6	1.81

was equipped with one Linear Variable Differential Transducer (LVDT) in the horizontal direction. An automated hydraulic actuator was horizontally installed along the desired direction at top floor. Quasi-static loads were applied at uniform rate to simulate structural damage.

2.2 Repair strategy of the frames

For repair of the seismically damaged frame, two commonly used FRP's namely unidirectional glass fiber reinforced polymer (GFRP) and unidirectional carbon fiber reinforced polymer (CFRP) were used with properties presented in Table 1. The thickness of GFRP sheet used is 0.34 mm whereas the thickness of CFRP sheet used is 1.2 mm. For retrofitting, low viscous epoxy (M Brace Master Injector 1319) was used first to fill the internal cracks using injection technique. M Brace putty 2200I was used for surface preparation after crack filling. After surface preparation, GFRP sheet was affixed by M Brace epoxy on the damaged joints at each floor and CFRP was used to retrofit the column hinge region in ground floor.

2.3 Performance of epoxy bonding of FRP with concrete

To examine the bonding ability of epoxy in crack filling, standard prism of 100mm×100mm×500 mm length were casted and tested in two point loading (Fig. 4).

Damaged prisms were reconnected using three different types bonding agents of cement slurry, M Brace 2200I and Master Injector 1315 epoxies. Two samples of each were tested. The reconnected samples were allowed to cure for a week and again tested in two points loading till failure (Fig.5). It is also important to investigate the performance of CFRP and GFRP to loads and also the effectiveness of the different binders used for bonding FRP's to concrete. For this standard prism of 100mm×100mm×500 mm length were cast and tested. A pair of control prisms and strengthened with GFRP and CFRP in tension zone are

Fig. 4 Control Beam

Fig. 5 Failure of Epoxy jointed Prisms

Fig. 6 FRP wrapped prisms

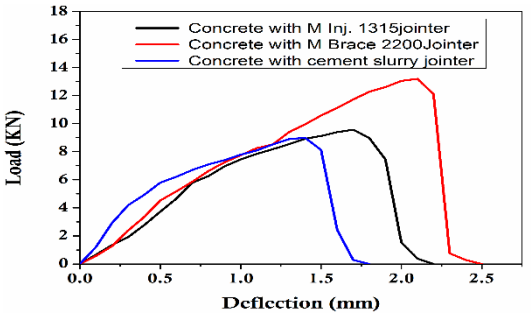

Fig. 7 Flexural strength of reconnected Prism specimens

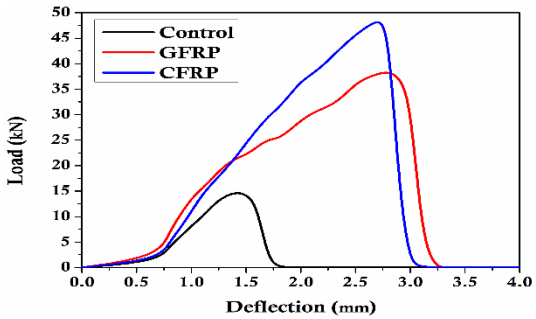

Fig. 8 Load Deflection behaviour of control and FRP repaired prisms

tested subjected to two points loading to estimate the load-deflection characteristics (Fig.6).

The load deflection behaviour of reconnected specimens shows the importance of bonding materials (Fig 7). The specimen with cement slurry recorded the least performance over the other epoxy reconnected specimens. Both the epoxy jointed specimens show different peak response with respect to the cement slurry jointed specimens. It proves that the epoxy injection will act as better bonding agent in creating the contact between cracked surfaces. The failure pattern was also supported the same trend. The M Brace 2200 jointer showed the best results and was further employed for repair of the RC frames.

From the load deflection behavior of prism specimens strengthened by FRP tested under two point loading (Fig. 8), it is observed that the FRP strengthened specimens show drastic improvement in the load-deformation characteristics as compared to control prisms. In particular, the specimen repaired at the bottom with higher modulus CFRP possesses better load carrying capacity and the crack appeared in the un-strengthened part pointing towards the efficiency of bonding. The specimen repaired with GFRP splits into two halves at mid-span and the experiment demonstrates the importance of higher modulus FRP in resisting load.

2.4 Vibration monitoring using impact hammer

Impact hammer test is an important tool to assess the health of a structure using vibration diagnostic technique. Impact hammer with a hard rubber tip was used to excite vibrations in the RC frames. Impact excitation was given at first, second and third floor respectively. Each floor of the RC frame was equipped with one accelerometer to measure the responses in axial direction. The control bare and masonry infilled frame as well as repaired frames were subjected to impact hammer testing to record the accelerations at different stages of loading. The signals from the accelerometers were acquired using Data Acquisition System. Fast Fourier Transform (FFT) spectrum analyzer based software (OROS-35) was used to analyze the signal. These vibration measurements predicted the different damage states with respect to specific frequencies.

2.5 Repair and retrofitting scheme

Initially the bare and brick infilled RC frames were tested to failure with loading as shown in Fig. 3. The failed and the deformed frames were restored again to their initial position using a hydraulic system. Damaged concrete was removed from the joint region and the surfaces were cleaned to remove dirt (Fig. 9a). All the corners of damaged elements were beveled and rounded to a radius of 10 mm in order to avoid corner stress concentration due to sharp edges on FRP. First the surface cracks were filled with M Brace 2200I putty (Fig. 9b) and then the surface was smoothened. Master injector 1319 was used to fill the internal cracks to create bond between the cracked regions in the damaged part of the frame (Fig. 9c). Two different FRP materials of GFRP and CFRP were used with M Brace epoxy (Fig. 9d). GFRP was used in the beam-column joint of every floors (Fig.9e) and CFRP was used to strengthen the column hinges (Fig.9f). The wrapping system of FRP

(a) Damaged Joint (b) Epoxy injection in internal crack (c) Restored Joint

(d) GFRP Strengthening (e) CFRP Strengthening (f) Retrofitted Beam Column

Fig. 9 Strategy for Retrofitting of Frame

sheets was followed in two steps: the first layer affixed perpendicular to the loading direction and second layer was wrapped to confine the existing layer in parallel direction. Stepwise strategy of FRP retrofitting followed for the frames is shown in Fig. 9.

The repaired and restored bare and brick infilled RC frames were again subjected to quasi- static loading and vibration monitoring was done by using impact hammer as explained above to compare the response of two frames.

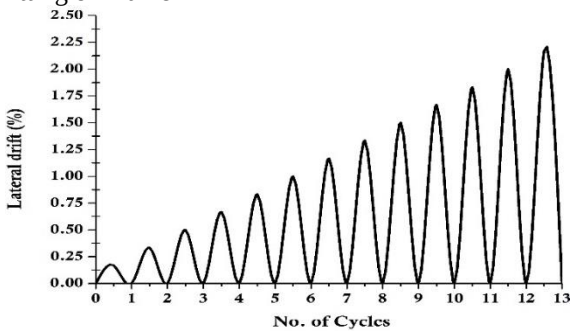

Fig. 10 Loading history

3. Results and discussion

3.1 Load-displacement behavior

The control scaled model frame was constructed and tested under quasi-static load. Load was applied by increasing deflection of 5mm in each cycle at the middle of top floor to simulate different levels of damage (Fig. 10). The hysteresis behavior/load – displacement of control and retrofitted bare frame and control and retrofitted brick-infilled frame are shown in Fig. 11 and Fig. 12 respectively. As the experiments were deflection controlled, so initially more load is required for little deflection due to stiffness of the frame. In Bare control frame Fig11(a) 2.82 kN load required for just 0.5 mm deflection whereas 5.74 kN load is required for 5mm deflection and In Bare retrofitted frame Fig. 11(b) 2.67 kN load required for just 0.5 mm deflection whereas 6.92 kN load is required for 5mm deflection. In Brick infilled control frame Fig12(a) 7.2 kN load required for just 0.5 mm deflection whereas 25.9 kN load is required for 5mm deflection and In Brick infilled retrofitted frame Fig. 12(b) 5.84 kN load required for just 0.5 mm deflection whereas 17.58 kN load is required for 5mm deflection. The comparison of the load displacement curves of control and retrofitted bare frames and control and retrofitted brick infilled frame are represented in Fig. 13. The load-displacement envelope curve is used to estimate the lateral deformation capacity (ductility) of the structure at different seismic performance levels and the corresponding force modification factor (R) of the structure as per based on FEMA guidelines are defined as: Linear Limit, Immediate Occupancy (IO), Damage Control (DC), Life Safety (LS), Limited Safety Structural Range (LSR), Collapse Prevention (CP), Collapsed(C) (Table 2, Fig.14).

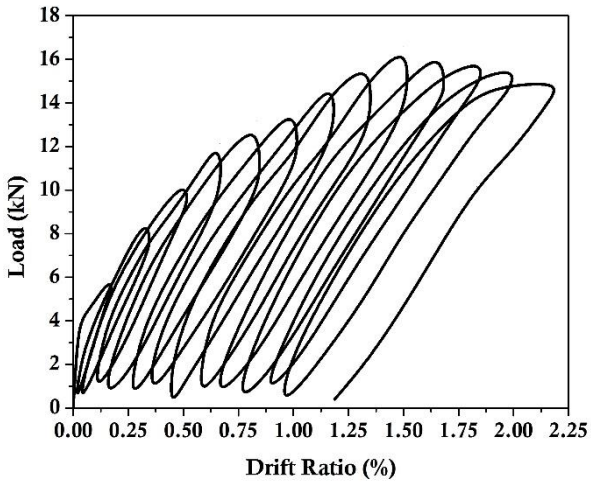

(a) Control Frame

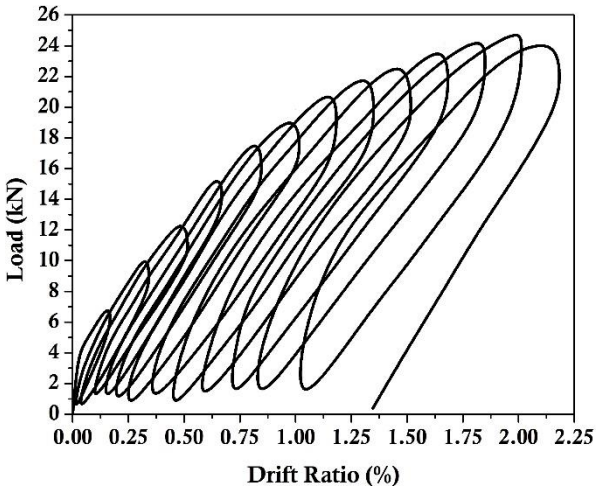

(b) Retrofitted Frame

Fig. 11. Hysteresis Loop of Bare Frame

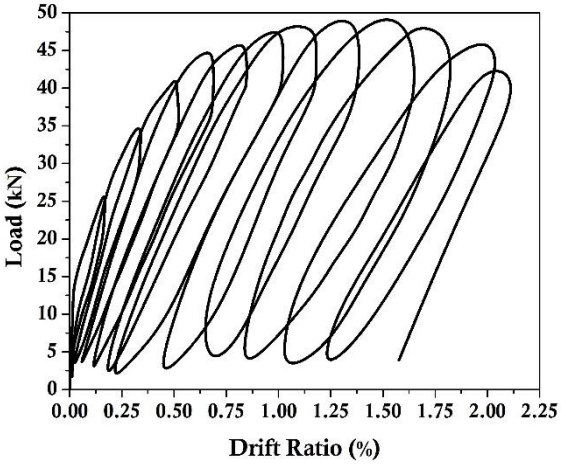

(a) Control Frame

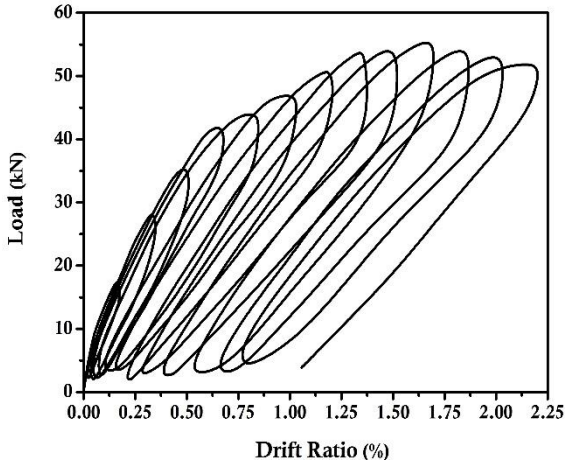

(b) Retrofitted Frame

Fig. 12. Hysteresis Loop of Brick Infilled Frame

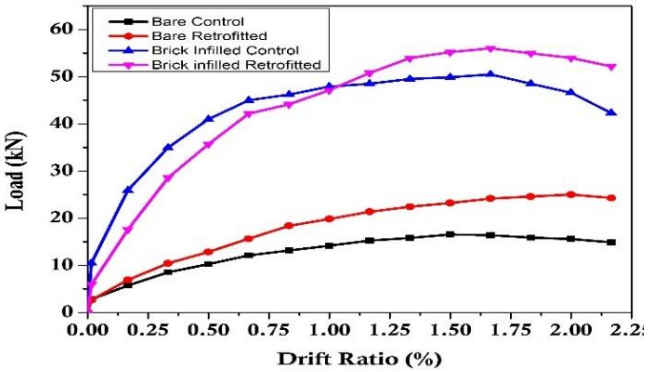

Fig. 13 Comparison of load deflection curves of Control and Repaired Bare and Brick in-filled frames

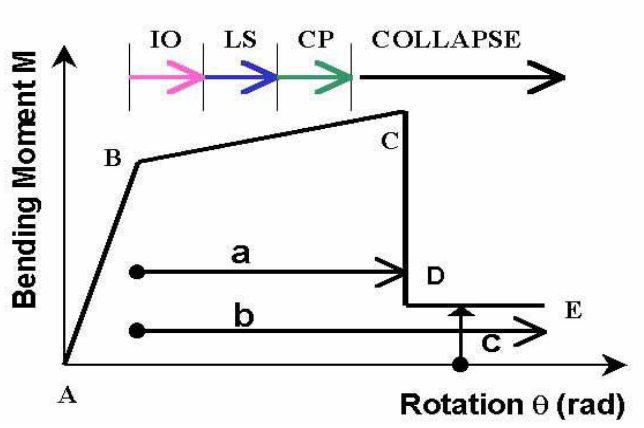

Fig. 14 Failure mechanism of structure as per FEMA-356 guidelines

Table 2 Performance Levels as per FEMA-356 guidelines

FEMA Performance Level	A-B	IO	DC	LS	LSR	CP	C
FEMA Damage Index	0	0.17	0.33	0.5	0.67	0.83	1

The initial part of the load-deformation curve shows linear behavior upto yield followed by non-linear behavior. In the bare frame, maximum load of 16.5 kN was attained at deflection of 45 mm in control and 24.6 kN load in

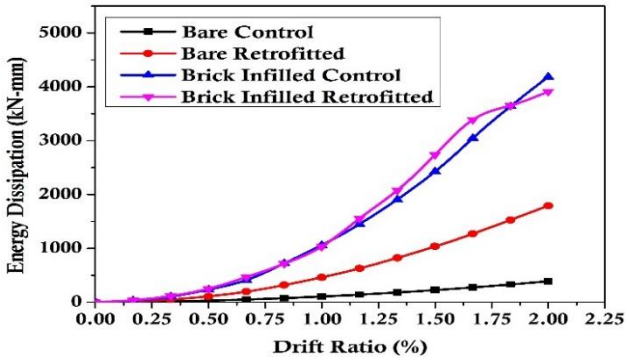

Fig. 15 Energy Dissipation V/s deflection of control and retrofitted frame

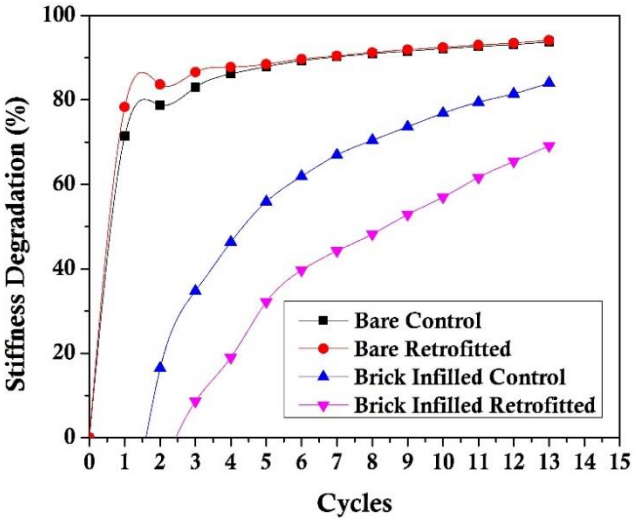

Fig. 16 Stiffness degradation of Control and Retrofitted Frames

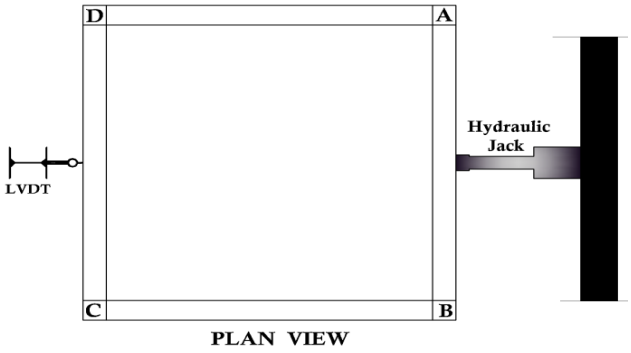

Fig. 17 Plan of the experimental model

retrofitted frame was attained at deflection of 55 mm. In brick infilled frame, maximum load of 49.5 kN was attained at 45 mm deflection in control frame and in retrofitted brick infilled frame, the load attained was 56.03 kN at 50 mm deflection. It points towards the effect of FRP confinement resistance to deformation. Also the peak load values indicate significant increase in the load carrying capacity of brick-infilled frames vis-à-vis bare RC frames (200%). It is a direct indicator of the confining effect of brick infills on a RC framed structure when subjected to axial loads.

Comparison of the hysteresis curves of both the types of bare and brick-infilled frames are distinct in terms of residual deflection. In both kinds of frames, the control frames show higher residual deflection than retrofitted specimens at same load. The retrofitted frames show reduced loop area during initial cycles due to the FRP confinement. As a result of the employed yielded reinforcement, the yield deflection is high and yield stiffness is low in retrofitted specimens than in control specimens. The retrofitted frames shows 51% and 30% higher load carrying capacity in corresponding bare and brick infilled frames and better post yield behavior even with yielded reinforcement. As the displacement increases, the cracks were formed above and below the strengthened region and hence reduction in load was noticed. But the concrete fails by crushing in the column hinge and joint diagonal cracks shows sudden decrease in load carrying capacity. This shows the structural behavior of all the frames was within LS to CP limits as per ASCE 41-06.

3.2 Energy dissipation

Energy dissipation is estimated by the area under the load deformation curve. Fig. 15 shows the energy dissipation curve of all the framed structures.

Energy dissipation capacity of the control bare frame is nominal in comparison to the retrofitted bare frame. The repaired frame shows enhanced energy dissipating capacity than the bare frame. The performances of control and retrofitted brick infilled frames were similar upto 50 mm deflection. As a result of severe cracking in the hinge region, the control frame failed to show better post peak load carrying capacity and a decrease in the energy dissipation capacity. On the other hand, in the retrofitted frame, no sudden failure is observed and better post peak performance is seen. The retrofitted frame shows gradual and increased energy dissipation capacity as compared to the control frame. On comparing bare and brick –infilled frames, brick infilled frame scores much higher energy dissipation capacities than the bare frames. Hence, it is important to model RC frames with infill walls as the stiffness behavior as well as the straining effect and the seismic demand is entirely modified due to composite frame-wall action.

3.3 Stiffness degradation

The difference between the initial and secant stiffness shows the post yield behavior of a structural component. In this study, the degradation in stiffness is calculated in terms of post elastic stiffness degradation over yield stiffness [represented by K deg%] using Eq. 4(Chidambaram and Aggarwal 2015):

$$K_{deg}\% = \left[1 - \frac{(K - K_y)}{K_y}\right] * 100 \qquad (4)$$

Where: K – Stiffness of each cycle, kN/mm; Ky –Yield stiffness, kN/mm

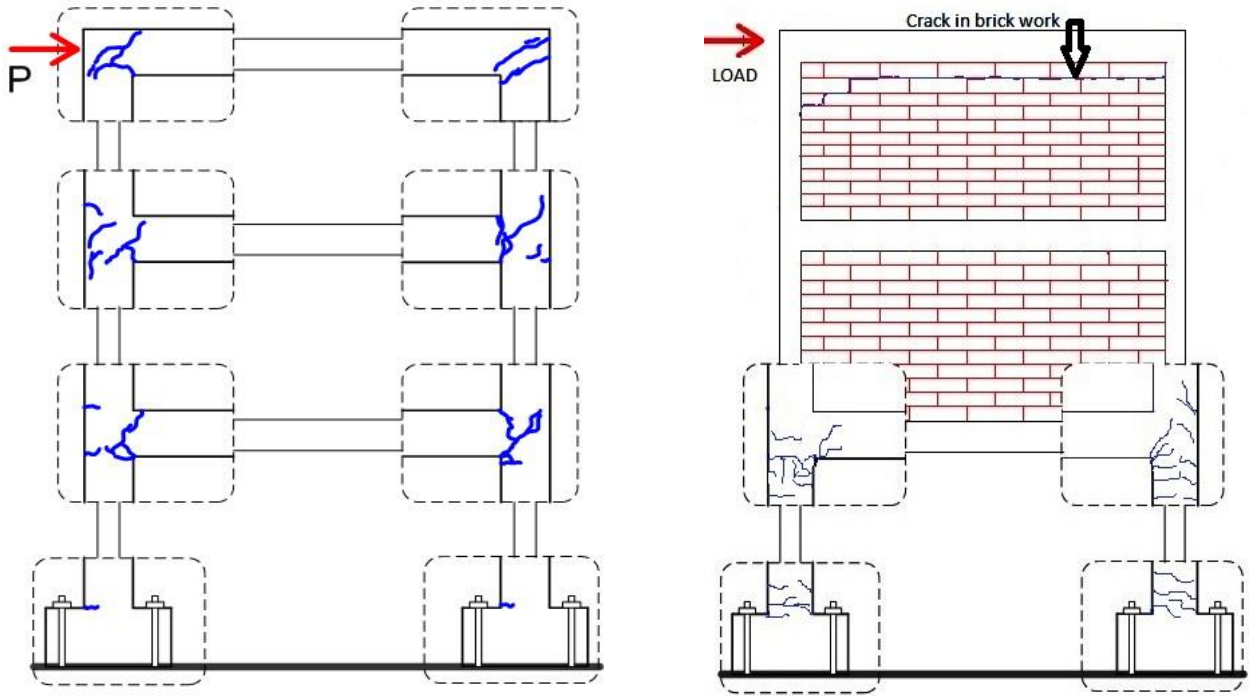

(a) Bare Frame (b) Brick infilled Frame

Fig. 18 Crack pattern observed in the frames

The rate of change of stiffness degradation over the post elastic range is the measure of inelastic performance of the component. The stiffness degradation post elastic drift for each tested frame specimen is plotted in Fig. 16. Sudden or rapid degradation in stiffness shows the brittle performance while low rate of stiffness degradation shows ductile performance. It is observed that bare frames undergo maximum degradation (upto 80%) in first few cycles indicating their behavior whereas in masonry infilled frames, rate of degradation is comparatively pointing towards their ductile behavior.

Also the comparison of control and retrofitted frames shows that initially the loss of yield stiffness was high in retrofitted specimens than control frames. This is because of the employed yielded reinforcement in the RC frame. In the damaged RC frame, the surface concrete in the impaired location has been thoroughly removed and replaced with epoxy putty and the internal cracks were injected with epoxy. But the reinforcement in the hinge region was not replaced and hence all the hinge regions were critically strengthened using external FRP reinforcement. Thus, the retrofitted specimens show higher loss in initial yield stiffness than control frame. But the post elastic stiffness degradation was comparatively low in retrofitted frame as compared to control frame. It illustrates the influence of external FRP strengthening in non-linear performance.

3.4 Crack pattern

The crack pattern was critically monitored and marked on the surface of the specimen during the testing. Four columns were marked as A, B, C, D for identification as shown in Fig 17.

In the bare RC frame, the plastic hinge was formed exactly below the first floor beam-column joint connection and at the column-foundation connection. Initially flexural cracks were noticed at the beam-column connection region followed by joint shear cracks. As the deformation increased widening of cracks was observed in each storey of bare frame whereas dense cracks were noticed at the foundation hinge region. Similar intensity of failures occurred at each storey of bare frame joints as depicted in Fig. 18a.

In the brick infilled frame, the infill in the first and second storey made the ground storey soft and hence the failure intensity was high in the ground storey as depicted in Fig18b. Predominant cracking was observed in the first floor beam-column joint region whereas the second floor and the roof depicted no evidence of cracking because of the soft storey effect. The horizontal cracking witnessed below the joint region reduced the stiffness and restricted the deformation capacity and was further followed by shear cracks in the joint region. As a result of the dense crack concrete cover, spalling occurred in the joint region. The effect of seismic detailing supports the RC frame to deform but the brittle nature of concrete exhibits concrete crushing failure at the foundation hinge region. There is no severe damage in the infill; horizontal sliding cracks were noticed in the infill at the mortar joints as shows in Fig. 19 (a-i).

In retrofitted frames, the internal cracks were injected with epoxy and after a thorough surface preparation, FRP wrapping was done. Thus, the failure pattern of the retrofitted frame is different from control frame. The FRP strengthening at the column hinge location and beam-column joint made strengthened portion stiffer and hence failure was concentrated in the un-strengthened region. The

(a) Cracks in Column A (b) Cracks in Column B (c) Cracks in Column C

(d) Cracks in Column D (e) Cracks in Column Hinge A (f) Cracks in Column Hinge B

(g) Cracks in Column Hinge C (h) Cracks in Column Hinge D (i) Cracks in Brick Infill

Fig. 19 Damage in Column-Beam and Column-Foundation after loading in control brick infilled frame

increase in unwrapping sound witnessed the failure of retrofitted frame by increasing the load. Fig. 20 (a-h) shows the cracks below and above the strengthened portion followed by FRP rupture in few locations. The primary failure is because of the horizontal crack below the FRP strengthened region. Thus the ultimate deformation of the repaired frame is identical with the control frame.

3.5 Park and Ang damage index

It is now generally accepted that the energy dissipated by structures during earthquakes has an effect on the level of the structural damage. Experiments on structural members and structures indicate that the excessive deformation and hysteretic energy are both the most important factors contributing to seismic damage. Hence, the damage models combining deformation ductility and hysteretic energy appear to be more reasonable. One of the best known and most widely used cumulative damage models is the Park-Ang model (Park and Ang 1985) as follows:

$$DI_{Park} = \frac{\delta_{\max}}{\delta_u} + \frac{\beta}{\delta_u P_y} \int dE_h \tag{5}$$

where $\delta_{\max}$ is the maximum experienced deformation; δ_u and P_y are the ultimate deformation under monotonic loading and yield strength of the structure respectively, which can be calculated using nonlinear finite element analysis; $\int dE_h$ is the hysteretic energy absorbed by the structural element during the response history; and β is a model constant parameter. This model has been well accepted owing to its simplicity and the fact that it has been calibrated against a significant amount of observed seismic damage. Although being the most widely used, the Park-Ang damage model does not converge at its upper and lower limits, that is: (1) damage index is greater than 0 when structures are loaded within elastic range, thus sustain no damage; (2) damage index is greater than 1.0 while structures are loaded monotonically to failure.

Park and Ang damage index is shown in Table 2 which clearly indicates that maximum damage was in control bare

(a) Retrofitted Column Hinge A (b) Column Hinge B (c) Retcrofitted Column Hinge C

(d) Retrofitted Column Hinge (e) Retrofitted Column A (f) Retrofitted Column B

(g) Retrofitted Column C (h) Retrofitted Column D

Fig. 20 Damage in Column-Beam and Column-Foundation after loading in Retrofitted Brick infilled frame

frame/retrofitted bare frame and control brick infilled frame and damage was minimum in retrofitted brick infilled frame. That was due to increase in stiffness by the brick infill and damage occurred in ground floor beam column joint was due to soft storey effect.

3.6 Damage Index based on load deflection behaviour

The damage tolerance capacity of the frames has also been estimated using the Damage Index (DI) based on load deflection (Fig. 21). It shows that as the displacement increases in every cycle, the damage increases. The brittle nature of concrete allows early crack formation in the hinge region. The damage index plot shows damage experienced by the bare frames is large in comparison to brick infilled frames. Also the damage experienced in control frames is larger than in retrofitted frames. The presence of FRP in the plastic hinge region of beam and column resist the load effectively without any crack in the joint. The cracks were initiated above and below the FRP strengthened region. The effective confinement of FRP allows the frame

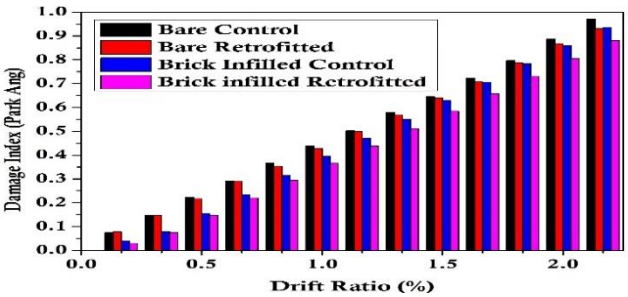

Fig. 21 Damage Index based on load deflection

deformations and restricts early joint failure. Thus its shows a damage index of 0.72 and 0.71 in control and retrofitted bare frame at 10^{th} cycle respectively whereas a DI of 0.71 and 0.66 is observed in control and retrofitted brick infilled frame at the same 10^{th} cycle. The DI of retrofitted frame shows sudden increase after 10^{th} cycle. This is possibly because of the occurrence of severe damage in the unconfined region and part of FRP rupture during larger deformation

Table 2 Damage index of Bare and Brick filled control and retrofitted frames (Park and Ang)

Cycles	Deflection (mm)	Bare Frame		Brick Infilled	
		Control	Retrofitted	Control	Retrofitted
	0	0	0	0	0
1st Cycle	5	0.07	0.08	0.04	0.03
2nd Cycle	10	0.15	0.15	0.08	0.07
3rd Cycle	15	0.22	0.22	0.16	0.15
4th Cycle	20	0.29	0.29	0.24	0.22
5th Cycle	25	0.37	0.35	0.31	0.29
6th Cycle	30	0.44	0.43	0.39	0.37
7th Cycle	35	0.50	0.49	0.47	0.44
8th Cycle	40	0.58	0.57	0.55	0.51
9th Cycle	45	0.65	0.64	0.63	0.58
10th Cycle	50	0.72	0.71	0.71	0.66
11th Cycle	55	0.80	0.78	0.78	0.73
12th Cycle	60	0.89	0.87	0.86	0.81
13th Cycle	65	0.97	0.93	0.94	0.88

Table 3 Natural Frequency, FRF, Damping and Damage index of Control Bare frame

	Cycle	P,kN	P/P_{max}	Natural frequency of each mode, Hz			FRF magnitude of each floor, 10-3 g/N			Damping	DI_{FRF}	Appearance
				ω_1	ω_2	ω_3	FRF_1	FRF_2	FRF_3			
0 Damage	0	0	0	6.6	19.5	31.8	2	3.6	4.8	3	0	Un-deformed
After 2 cycles	2	5	0.3	6.4	19	30.5	0.6	1.2	1.8	3.42	0.09	Un-cracked
After 4 cycles	4	7.5	0.45	6.1	18	29	0.5	1.1	1.5	3.77	0.18	Un-cracked
After 7 cycles	6	10	0.61	5.8	17.5	28	0.4	1	1.25	4.15	0.32	Minor cracking
After 10 cycles	8	12.5	0.76	5.5	17	27.2	0.46	0.9	1.2	4.67	0.49	Severe cracking
After 13 cycles	10	16.5	1	5.2	15.5	25.8	0.3	0.6	1	5.21	0.95	Loss of shear capacity

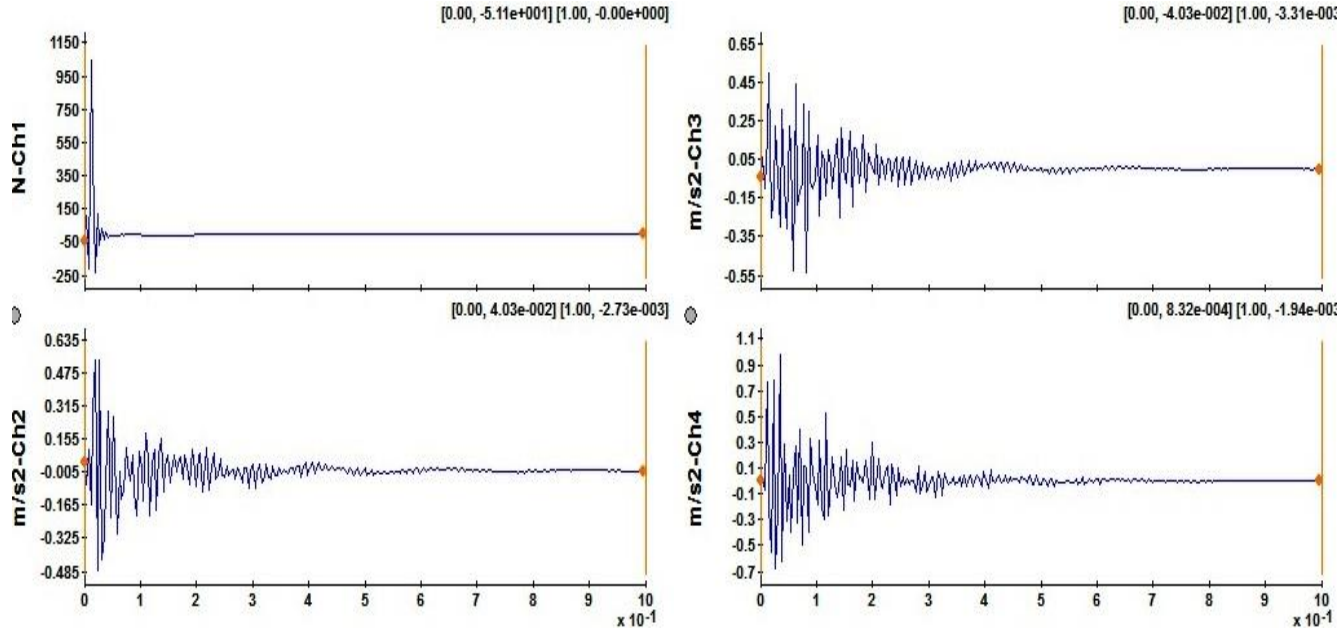

Fig. 22 Trigger block

Table 4 Natural Frequency, FRF, Damping and Damage index of Retrofitted Bare frame

	Cycle	P,kN	P/P_{max}	Natural frequency of each mode, Hz			FRF magnitude of each floor, 10-3 g/N			Damping	DI_{FRF}	Appearance
				ω1	ω2	ω3	FRF_1	FRF_2	FRF_3			
0 Damage	0	0	0	6.7	20.7	34.3	3	6.5	8.4	3.07	0	Un-deformed
After 2 cycles	2	6	0.24	6.5	20.3	33.5	1.3	3.1	3.9	3.12	0.06	Un-cracked
After 4 cycles	4	12	0.48	6.4	20	32.6	1	2.7	3.6	3.93	0.14	Un-cracked
After 6 cycles	6	15	0.6	6.2	19.5	32.2	0.8	1.9	2.5	4.11	0.18	Un-cracked
After 8 cycles	8	18	0.72	6.1	19.3	32	0.6	1.3	1.8	4.46	0.24	Sound of fiber slip
After 10 cycles	10	21	0.84	6	18.8	31.5	0.6	1.5	2	5.11	0.32	Sound of breaking fiber
After 13 cycles	13	25	1	5.5	17.2	29	0.5	1.2	1.5	6.09	0.88	Loss of shear capacity

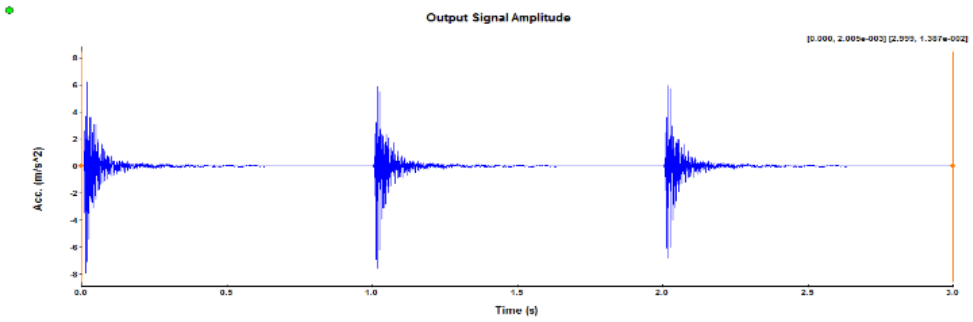

Fig. 23 Time History Plot

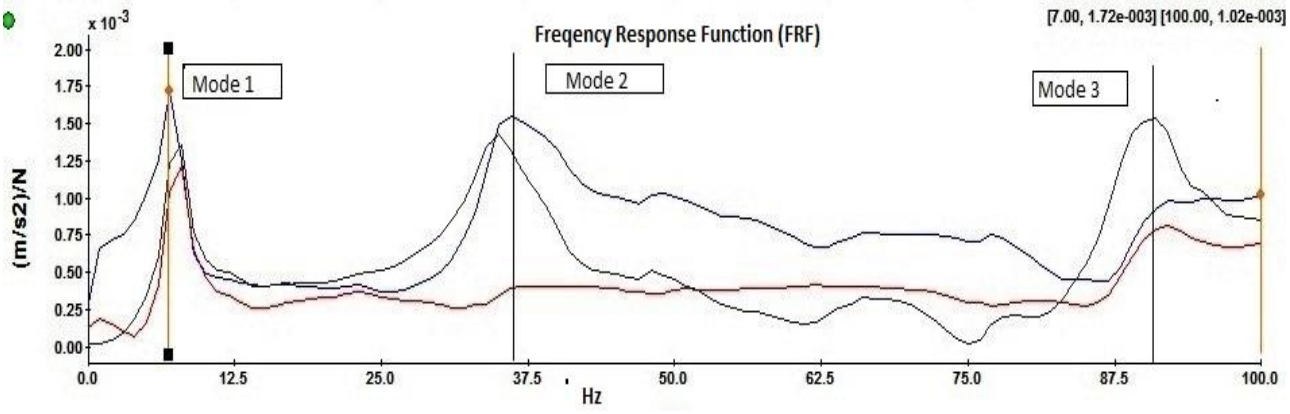

Fig. 24 Frequency Response Function for Control Brick Infilled Frame

3.7 Dynamic characteristics

As discussed, the dynamic characteristics of the RC frames were measured using Impact hammer testing. The frames were subjected to impact excitation at center of beam at all storeys and the response at all different storeys was measured using accelerometer at different stages of loading. The signals from the accelerometers were acquired using Data Acquisition System. Fast Fourier Transform (FFT) spectrum analyzer based software (OROS-35) was used to analyze the signal and was plotted as FRF (Frequency Response Function). These vibration measurements predicted the different damage states with respect to specific frequencies. FRF based damage index is one of most effective way to relate to the health of the structure at different stages of damage. The change in fundamental frequency and magnitude of FRF of a system defines the damage behavior. Fig. 22 represents trigger block plot representing the excitation force when the frame was subjected to an impact hit (Fig. 22a) and Fig. 22(b-d) gives the corresponding response given by the accelerometer at each storey. Time History plot is shown in Fig. 23 which indicates acceleration of vibration of each storey. The vibration response in the form of FRF plot is shown in Fig. 24.

Table 5 Natural Frequency, FRF, Damping and Damage index of Control Brick infilled frame

	Cycle	Load (KN)	P/P (Max)	Natural frequency of each mode, Hz			FRF magnitude of each floor, 10-3 g/N			Damping	DI_{FRF}	Appearance
				ω1	ω2	ω3	FRF1	FRF2	FRF3			
0 Damage	0	0	0.00	7	39.8	79.7	3.967	5.038	6.262	0.250	0	Un-deformed
After 2 cycles	2	35	0.71	6.9	38.4	79.1	3.718	4.732	5.838	0.258	0.063	Un-deformed
After 4 cycles	4	45	0.91	6.7	37.2	78.4	3.324	4.193	5.24	0.321	0.162	Un-cracked
After 6 cycles	6	47.9	0.97	6.4	36.8	77.7	2.741	3.491	4.38	0.351	0.309	Un-cracked
After 8 cycles	8	49.5	1.00	5.9	36.3	76.8	2.077	2.641	3.283	0.373	0.476	Minor cracking
After 10 cycles	10	48.5	0.98	5.2	35.9	76.2	1.367	1.757	2.143	0.385	0.655	cracking
After 13 cycles	13	41.3	0.83	4.8	35.2	75.9	0.666	0.916	1.159	0.412	0.832	Loss of shear capacity

Table 6 Natural Frequency, FRF, Damping and Damage index of Retrofitted brick infilled frame

	Cycle	Load (KN)	P/P(Max)	Natural frequency of each mode, HzFRF magnitude of each floor, 10-3 g/N						Damping	DI_{FRF}	Appearance
				ω1	ω2	ω3	FRF1	FRF2	FRF3			
0 Damage	0	0	0.00	7.6	44.7	89.1	3.794	4.156	6.028	0.257	0	Un-deformed
After 2 cycles	2	28.58	0.51	7.2	42.3	86.4	3.578	3.922	5.686	0.283	0.057	Un-cracked
After 4 cycles	4	42.19	0.75	7	39.7	84.3	3.27	3.553	5.182	0.341	0.138	Un-cracked
After 6 cycles	6	47.14	0.84	6.7	37.4	81.7	3.03	3.141	4.676	0.363	0.201	Un-cracked
After 8 cycles	8	53.94	0.96	6	36.9	78.5	2.428	2.577	3.711	0.378	0.36	Sound of fiber slip
After 10 cycles	10	56.03	1.00	5.4	36.2	76.9	1.819	1.935	2.805	0.394	0.521	Sound of breaking fiber
After 13 cycles	12	53.98	0.96	4.8	35.7	76	0.812	0.978	1.387	0.429	0.786	Loss of shear capacity

The frequencies and the corresponding distribution of amplitude are global properties. The observed natural frequencies and the estimated damage index calculated with reference to drop in FRF magnitude (Vimuttasoongviriya et.al. 2009) are presented in the Table 3 for control bare frame, in Table 4 for retrofitted bare frame, in Table 5 for control brick infilled frame and Table 6 for retrofitted brick infill frame.

The conventional and retrofitted frame shows similar kind of frequency response. The test results shows reduction in the natural frequency as the damage level increases. The control specimens show natural frequencies ranging from 6.6 - 5.2 Hz with change in DI from 0 to 0.95 for bare frames and 7- 4.8Hz with the change in DI from 0 to 0.832 in brick infilled frame. On the other hand, natural frequency ranges from 6.7 – 5.5 Hz with change in DI from 0 to 0.88 for retrofitted bare frame and 6.6 – 4.8 Hz with change in DI from 0 to 0.66 for retrofitted brick infill frames shown in Fig 25.

The natural frequency reduces as the damage level increases and it shows 31.4 % reduction in natural

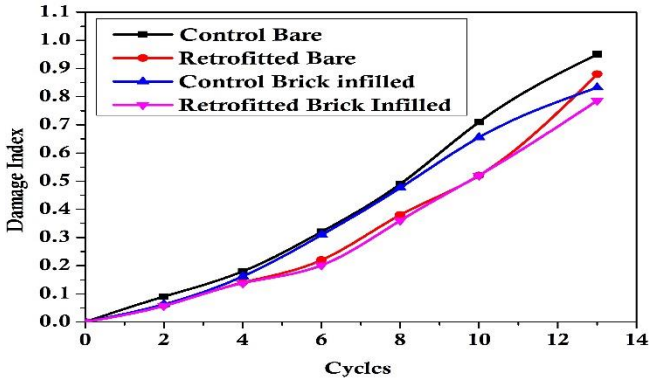

Fig. 25 Damage Index Based on Vibration Monitoring

frequency at failure stage. The FRF magnitude is found to decrease and damping ratio is found to increase with the increase in deformation. Thus the conventional frame shows 67% and 69% reduction in FRF magnitude and 74% and 64 % increase in damping ratio in bare frame and brick infill frame respectively.

The retrofitted frame specimen shows similar trend to conventional frame with respect to frequency response. The observed natural frequency of conventional specimen varies from 6.7 to 5.5Hz with the change in damage index from 0 to 0.88. It shows 36.8 % reduction in natural frequency at failure stage. This proves the effectiveness of the strengthening technique adopted in restoring the frame. There was a tremendous change in FRF magnitude and damping ratio shows remarkable energy dissipation capacity of the retrofitted frame as compared to conventional frame. The observed FRF reduction of the retrofitted frame is 66.2% and 72% increase in damping ratio.

4. Conclusions

This experimental study mainly focuses on comparison of investigation of bare and brick infilled control and retrofitted frames under cyclic loading. The hysteretic curve, stiffness retention, energy dissipation, damage tolerance and failure pattern are the main parameters used in this study to examine the efficiency. Following are the main conclusions derived:

1. There is a significant improvement in load carrying capacity of brick infilled frame over bare frame and FRP strengthened brick infilled frame over bare frame under bending. During the bending test it was found that reconnected points sustained and crack was found below the load point. It proves the effectiveness of epoxy in bonding.

2. Hysteresis behavior of FRP repaired bare as well as brick infilled RC frame under cyclic loading shows better post yield behavior and enlarged loop area. Also the residual deflection is lesser than control specimen due to better damage tolerance. It shows that the FRP strengthened frame offers better elastic and inelastic behaviour.

3. The employed existing yielded reinforcement failed to show better initial and yield stiffness than control specimen. Even though with lesser initial stiffness the retrofitted frame provides better post yield stiffness retention as compared to control specimen. This kind of retrofitting and FRP strengthening may be an effective method in restoring the structural integrity.

4. The enlarged loop area shows better dissipated energy level and damage tolerance capacity of adopted strengthening technique in the retrofitted frame. The dynamic test also proves the same trend in damage tolerance. The crack pattern and failure behavior shows that the strengthened portion behaves more sustainable than unstrengthen region. Thus the failure mainly concentrated in the weakest portion of the frame. But the FRP strengthening in the hinge region supports the frame to provide better inelastic deformation.

5. Under cyclic load in bare frame damage occurs in all stories while in brick infilled frame, only soft storey showed maximum damage. Little damge was observed in brick infills which show that brick infill makes the building stiffer and stronger as compared to bare frame.

References

Beydokhty, E.Z. and Shariatmadar, H. (2016), "Behavior of damaged exterior RC beam-column joints strengthened by CFRP Composites", *Lat. Am. J. Solids Struct.*, **13**(5), 880-896. https://doi.org/10.1590/1679-78252258.

Ceroni, F. (2010), "Experimental performances of RC beams strengthened with FRP materials", *Construct. Build. Mater.,* **24**(9), 1547-1559. https://doi.org/10.1016/j.conbuildmat.2010.03.008.

Chang, S.Y., Li, Y.F. and Loh, C.H. (2004), "Experimental study of seismic behaviors of as-built and carbon fiber reinforced plastics repaired reinforced concrete bridge columns", *J. Bridge Eng.*, **9**(4), 391-402. https://doi.org/10.1061/(ASCE)1084-0702(2004)9:4(391).

Chidambaram, R.S. and Aggarwal, P. (2015), "Flexural and shear behavior of geo-grid confined RC beams with steel fiber reinforced concrete", *Construct. Build. Mater.,* **78**, 271-280. https://doi.org/10.1016/j.conbuildmat.2015.01.021.

Cho C., Ha G. and Kim, Y. (2008), "Nonlinear model of reinforced concrete frames Retrofitted by in-filled HPFRCC walls", *Struct. Eng. Mech.,* **30**(2), 211-223. https://doi.org/10.12989/sem.2008.30.2.211.

Dipasquale, E. and Cakmak, A.S. (1990), "Seismic damage assessment using linear models", *Soil Dynam. Earthq. Eng.*, **4**(9), 194-215. https://doi.org/10.1016/S0267-7261(05)80010-7.

Ghatte, H.F., Comert, M., Demir, C. and Ilki, A. (2015), "Seismic performance of full-scale frp retrofitted substandard rectangular rc columns loaded in the weak direction", Conference ACE 2015, Vietri sul Mare, Italy, June.

Goyal, A. (2007), "Structural Health Monitoring of Retrofitted RCC Beams using Vibration Measurements", M.Sc. Dissertation, Thapar University, Patiala, India.

Kanwar, V., Kwatra, N., Aggarwal, P. and Gambir, M.L. (2006), "Vibration Monitoring of a RCC Building Model", *Proceedings of National Conference on Technology for Disaster Mitigation*, Hamirpur, India, 277-285.

Kanwar, V., Kwatra, N. and Aggarwal, P. (2007), "Damage Detection for Framed RCC Buildings using ANN Modelling." *J. Damage. Mech.*, **16**(4), 457-472. https://doi.org/10.1177/1056789506065939.

Kanwar, V., Singh, Ramesh P., Kwatra, N and Aggarwal, P. (2016) "Monitoring of RCC structures affected by earthquakes", *Geomatics, Natural Hazards Risk.*, **7**(1), 37-64. https://doi.org/10.1080/19475705.2013.866984.

Ko, J.M., Sun, Z.G. and Ni, Y.Q. (2002), "Multi-Stage Identification Scheme for Detecting Damage in Cable Stayed Kap Shui Mun Bridge", *Eng. Struct.*, **24**, 857-868. https://doi.org/10.1016/S0141-0296(02)00024-X.

Lakshmikandhan, K.N., Sivakumar, P. and Ravichandran R. (2012), "Damage Assessment and Strengthening of Reinforced Concrete Beams", *J. Mater. Mech. Engg*., **2**(2), 34-42.

Maia, N.M.M., Silva, J.M.M., Almas, E.A.M. and Sampaio, R.P.C. (2003), "Damage Detection in Structures: from Mode Shape to Frequency Response Function Methods", *Mech. Syst. Signal Process.*, **17**(3), 489-498. https://doi.org/10.1006/mssp.2002.1506.

Rao, J.S. (2000), *Vibratory Condition Monitoring of Machines*, Narosa Publishing House, New Delhi, India.

Vimuttasoongviriya, A., Kwatra, N. and Kumar, M. (2009), "Effect of Lateral Quasi-Static Load on Nonlinear Behaviour and Damage Indexes of Retrofitted RC Frame Model", *Asian J. Civil Eng.*, **10**(5), 563-588.

Lakshmikandhan, K.N., Sivakumar, P. and Ravichandran, R. (2012), "Cyclic Load Performance Evaluation of Reinforced Concrete Beam and Repaired Concrete Beam", SERC Research Report No. CAD/OLP 14441/RR-(15).

Lakshmikandhan, K.N., Sivakumar, P. and Ravichandran, R. (2013), "Damage Assessment and Strengthening of Reinforced Concrete Beams", *Int. J. Mat. Mechl. Engg.,* **2**(2), 34-42.

Maia, N.M.M., Silva, J.M.M., Almas, E.A.M. and Sampaio, R.P.C. (2003), "Damage Detection in Structures: from Mode Shape to Frequency Response Function Methods", *Mech. Syst. Signal Process.*, **17**(3), 489-498. https://doi.org/10.1006/mssp.2002.1506.

Memon, M.S. and Sheikh, S.A. (2005), "Seismic Resistance of Square Concrete Columns Retrofitted with Glass-Fiber Reinforced Polymer", *ACI Struct. J.*, **102**(5), 774-783.

Massumi, A. and Mohammadi, R. (2016), "Structural redundancy of 3D RC frames under seismic excitations," *Struct. Eng. Mech.*, **59**(1), 15-36. http://dx.doi.org/10.12989/sem.2016.59.1.015.

Mukherjee, A. and Joshi, M. (2005), "FRPC Reinforced Concrete Beam-Column Joints under Cyclic Excitation", *Composite. Str.,* **70**, 185-199.

Mukherjee, A., Boothby, T.E., Bakis, C.E., Joshi, M.V. and Maitra, S.R. (2004), "Mechanical behavior of fiber reinforced polymer wrapped concrete columns-complicating effects", *J. Composite. Constr.*, **8**(2), 97-103.

Omar, A. and Stefan, K. (2014), "Modelling of circular concrete columns with CFRP sheets under monotonic loads by ATENA-3D", *Forecast Engineering: Global Climate Change and the Challenge for Built Environment*, Weimar, Germany, August. 1-15.

Ozkaynak, H., Yuksel, E., Yalcin, C., Dindar, A.A. and Buyukozturk, O. (2014), "Masonry infill walls in reinforced concrete frames as a source of structural damping", *Earthq. Engng. Struct. Dyn.,* **43**, 949-968. https://doi.org/10.1002/eqe.2380.

Park, Y.J. and Ang, A.H.S. (1985), "Seismic damage analysis of RC buildings", *Strl. Engg. (ASCE)*, ST4-111, 740-757. https://doi.org/10.1061/(ASCE)0733-9445(1985)111:4(740).

Rao, J.S. (2000), *Vibratory Condition Monitoring of Machines*, Narosa Publishing House, New Delhi, India.

Sathiaseelan, P. and Arulselvan, S. (2015), "Influence of Ferro Cement Retrofit in the stiffened in the fill RC frame", *Ind. J. Sci. Tech*., **8**(30),1-6. https://doi.org/10.17485/ijst/2015/v8i30/55058.

Singh, B., Chidambaram, R.S., Sharma, S., Kwatra, N. (2017), "Behavior of FRP strengthened RC brick in-filled frames subjected to cyclic loading", *Struct. Eng. Mech.*, **64**(5), 557-566. https://doi.org/10.12989/sem.2017.64.5.557.

Tunaboyu, O. and Avsar, O. (2017), "Seismic repair of captive-column damage with CFRPs in substandard RC frames", *Struct. Eng. Mech.*, **61**(1), 1-13. https://doi.org/10.12989/sem.2017.61.1.001.

Vimuttasoongviriya, A., Kwatra, N. and Kumar, M. (2009), "Effect of Lateral Quasi-Static Load on Nonlinear Behaviour and Damage Indexes of Retrofitted RC Frame Model", *Asian. J. Civil. Engg*., **10**(5), 563-588.

Vimuttasoongviriya, A., Kwatra, N. and Kumar, M. (2010), "Damage Detection of Strengthened RC Frame Model with FRP Sheets under Lateral Loads", *Proc., 11th Int. Conf. on Structures under Shock and Impact.* Tallinn, Estonia, 55-67.

Vimuttasoongviriya, A., Kwatra, N. and Kumar, M. (2010), "Modal Parameters Damage Method for Detecting Damage in Strengthened RC Frame Model using GFRP Laminate", *Proc., 15th National Conference in Civil Engineering*. Ubonratchathani, Thiland, STR2.

Vimuttasoongviriya, A., Kwatra, N. and Kumar, M. (2010), "Nonlinear Behaviour and Vibration Based Damage Identifation of Retrofitted RC Frame Model", *Proc., 9th Int. Conference for Highrise Towers ad Tall Building*. Munich, Germany, Paper No. 0958.

Vimuttasoongviriya, A., Kwatra, N. and Kumar, M. (2011), "Vibration monitoring and damage assessment of a retrofitted RC frame model", *KMITL Sci. Tech. J.*, **11**, 43-53.

Wang, Yung-Chih and Hsu, K. (2009), "Design recommendations for the strengthening of reinforced concrete beams with externally bonded composite plates", *Compos. Struct.,* **88**(2), 323-332. https://doi.org/10.1016/j.compstruct.2007.12.001.

Yao, G.C., Chang, K.C. and Lee, G.C. (1992), "Damage diagnosis of steel frames using vibrational signature analysis", *J. Eng. Mech.*, **118**(9), 1949-1961.

Yang, Y., Liu, R., Xue, Y. and Lu, H. (2017), "Experimental study on seismic performance of reinforced concrete frames Retrofitted with eccentric buckling-restrained braces (BRBs)", *Earthq. Struct.,* **12**(1), 79-89. https://doi.org/10.12989/eas.2017.12.1.079.

Yuksel, E., Ozkaynak, H., Buyukozturk, O., Yalcin, C., Dindar, A.A., Surmeli, M., Tastan, D. (2010), "Performance of alternative CFRP retrofitting schemes used in infilled RC frames", *Construct. Build. Mater.,* **24**, 596–609. https://doi.org/10.1016/j.conbuildmat.2009.09.005.

Zhu X.Q. and Law S.S. (2007), "A concrete–steel interface element for damage of reinforced concrete structures", *Eng. Struct*., **29**, 3515–3524. https://doi.org/10.1016/j.conbuildmat.2009.09.005.

CC